Sudden Relaminarization and Lifetimes in Forced Isotropic Turbulence

Moritz F. Linkmann* and Alexander Morozov
SUPA, School of Physics and Astronomy, University of Edinburgh, JCMB, King's Buildings, Peter Guthrie Tait Road EH9 3FD, Edinburgh, United Kingdom
(Received 6 May 2015; published 23 September 2015)

We demonstrate an unexpected connection between isotropic turbulence and wall-bounded shear flows. We perform direct numerical simulations of isotropic turbulence forced at large scales at moderate Reynolds numbers and observe sudden transitions from a chaotic dynamics to a spatially simple flow, analogous to the laminar state in wall bounded shear flows. We find that the survival probabilities of turbulence are exponential and the typical lifetimes increase superexponentially with the Reynolds number. Our results suggest that both isotropic turbulence and wall-bounded shear flows qualitatively share the same phase-space dynamics.

DOI: 10.1103/PhysRevLett.115.134502 PACS numbers: 47.27.Cn, 05.65.+b, 47.27.De, 47.27.Gs

Recent years have seen significant advances in our understanding of the transition to turbulence in wall-bounded shear flows. In simple geometries, like flow in a pipe or a channel, close to the transition threshold, a finite-amplitude perturbation develops into a localized turbulent patch (a "puff" in pipe flow) that exists as an independent entity [1–8]. Experiments [9,10] and numerical simulations [11–13] have shown that the localized patches of turbulence can spontaneously disappear (relaminarize) or split into two. The rates of these competing processes depend strongly on the Reynolds number: at relatively low Reynolds numbers it is much more probable for a puff to decay than to split, while the opposite is true at higher Reynolds numbers. The point where the two probabilities are equal marks the transition to a sustained turbulence [10], and the turbulence below this threshold may consist of long-lived chaotic transients [14]. The transition to turbulence in wall-bounded flows is thus intimately related to the process of relaminarization, where turbulent dynamics suddenly collapse to a much simpler, typically linearly stable, laminar state. Such events have been explained by dynamical systems theory as the escape from a chaotic saddle in state space with a constant (time independent) rate of escape [15–19]. At higher Reynolds numbers, spatially local relaminarization attempts [20,21] can be the source of intermittency in turbulent flows.

In contrast, stationary isotropic turbulence, which can be thought of as a turbulent flow far away from boundaries [22], is believed to exhibit much simpler dynamics: its motion is turbulent for all Reynolds numbers and there is no actual transition. In this Letter we report an unexpected connection between these two fields. We perform direct numerical simulations (DNS) of stationary isotropic turbulence at low Reynolds numbers and observe sudden breakdowns of the turbulent dynamics in favor of a much simpler state. Similar observations have been made in connection to symmetry breaking in isotropic turbulence [23] and in magnetohydrodynamic flows subject to electrical forcing [24]. We study the nature of this process and show that it is analogous to the relaminarization events in wall-bounded parallel shear flows. We find that forced isotropic turbulence at relatively low Reynolds numbers is transient and the rate of its collapse is constant in time, resulting in exponentially distributed lifetimes of the turbulent state similar to pipe [9,10,13,17] and plane Couette flow [11,25,26].

We perform direct numerical simulations of the incompressible Navier-Stokes equations

$$\partial_t \boldsymbol{u} = -\boldsymbol{\nabla} P - \boldsymbol{u}\cdot\boldsymbol{\nabla}\boldsymbol{u} + \nu\Delta\boldsymbol{u} + \boldsymbol{f}, \tag{1}$$

$$\boldsymbol{\nabla}\cdot\boldsymbol{u} = 0, \tag{2}$$

where $\boldsymbol{u}$ denotes the velocity field, $\boldsymbol{f}$ is an external force, ν is the kinematic viscosity, P is the pressure, and we set the density to unity. These equations were solved numerically using the standard fully dealiased pseudospectral method [27] on a 3D periodic domain of length $L_{\mathrm{box}} = 2\pi$ with the smallest wave number being $k_{\mathrm{min}} = 2\pi/L_{\mathrm{box}} = 1$. All simulations are well resolved, using 32^3 collocation points and satisfying $k_{\mathrm{max}}\eta \geq 1.82$, where η denotes the Kolmogorov dissipation scale.

The system is forced at large scales by a negative damping $\boldsymbol{f}$ defined as

$$\begin{aligned}\hat{\boldsymbol{f}}(\boldsymbol{k},t) &= (\varepsilon_W/2E_f)\hat{\boldsymbol{u}}(\boldsymbol{k},t), \quad \text{for } 0 < |\boldsymbol{k}| < k_f,\\ &= 0, \qquad \text{otherwise.}\end{aligned} \tag{3}$$

Here, $\hat{\boldsymbol{f}}(\boldsymbol{k},t)$ is the Fourier transform of the forcing, $\hat{\boldsymbol{u}}(\boldsymbol{k},t)$ is the Fourier transform of the velocity field $\boldsymbol{u}(\boldsymbol{x},t)$, E_f is the total energy contained in the forcing band, and $k_f = 2.5$ is the highest wave number forced. Normalizing the energy input by E_f ensures that the energy injection rate is

 © 2015 American Physical Society

$\varepsilon_W = \text{const}$; here we choose $\varepsilon_W = 0.1$. This forcing provides an energy input that does not prefer any particular direction and has a complicated, time-dependent spatial profile; note that $k_f = 2.5$ corresponds to 80 possible wave vectors and thus 80 different velocity field modes are being forced. It is commonly used in numerical investigations of homogeneous isotropic turbulence [28–34], the prime example being the series of high-resolution simulations of Kaneda *et al.* [35].

The initial conditions for the velocity with a prescribed energy spectrum are constructed by assigning a Gaussian random vector to each point in space. The resulting field is subsequently Fourier transformed and rescaled according to the desired energy spectrum in the form

$$E(k) = 0.001702k^4 e^{-2(k/5)^2}. \quad (4)$$

Further details of the numerical method, validation, and benchmarking of the code can be found in Ref. [27].

The simulations are evolved for 1271 initial large-eddy turnover times $t_0 = L/U$, where U denotes the initial rms velocity and L is the initial integral length scale; $t_0 = 0.78$ in simulation units. The parameter that is varied in our simulations is the viscosity ν, and we present the results in terms of a system-scale Reynolds number $\mathrm{Re} = L_{\mathrm{box}}^{4/3}\varepsilon_W^{1/3}/\nu$ that is changed from 53.80 to 97.82 for different simulations; in each individual run, Re is kept constant during the whole simulation. The corresponding values of the Taylor-Reynolds number and further simulation details are given in Supplemental Material [36].

As mentioned above, the form of the forcing term that we employ here [Eq. (3)] is routinely used in DNS of isotropic turbulence as its complicated spatial form would seem to guarantee that the system is turbulent at any Reynolds number larger than unity. Indeed, even at sufficiently low Reynolds numbers, we observe that our simulations reach a turbulent stationary state, where the energy injection is balanced by the average dissipation and there is motion at all length scales. Surprisingly, however, after staying in this steady state for a long time, the system exhibits a transition to a different state, as shown, for example, in Fig. 1 for $\mathrm{Re} = 76.86$. There, we plot the total energy of the system $E(t) = \int_{k_{\min}}^{k_{\max}} dk E(k,t)$ and the energy content of the small scales $E'(t) = \int_{k>k_{\min}}^{k_{\max}} dk E(k,t)$ as a function of time; the energy content at a particular length scale is $E(k,t) = |\hat{\boldsymbol{u}}(k,t)|^2/2$ and the largest scale in the system corresponds to $k_{\min} = 2\pi/L_{\mathrm{box}} = 1$.

As Fig. 1 demonstrates, turbulent dynamics persists until about $t/t_0 \approx 240$. After that, the total energy becomes constant and the small-scale fluctuations in the kinetic energy produced by the characteristic turbulent cascade process suddenly disappear. This implies that for $t/t_0 > 240$ the kinetic energy is confined to the largest scale of the system and no nonlinear transfer exciting the smaller scales takes place. The system thus transitions from a turbulent to a large-scale "laminar" state.

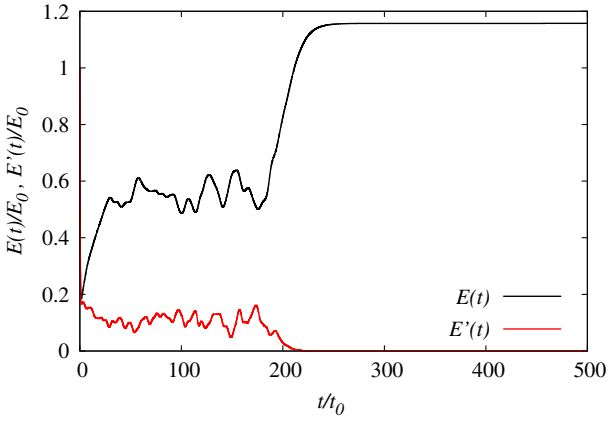

FIG. 1 (color online). Time evolution of the total energy $E(t)$ and the energy content of the small scales $E'(t)$ for $\mathrm{Re} = 76.86$ normalized by the initial energy E_0. Time is given in units of initial large eddy turnover time $t_0 = L/U$, where U is the initial rms velocity and L the initial integral scale. The point around $t/t_0 \approx 240$ when $E'(t)$ vanishes and the total energy becomes constant marks the onset of the self-organized state as discussed in the main text.

The existence of such a state can be understood if one considers a model velocity field with $u_x \sim \cos(y)$ and all other components of the velocity being zero. This flow profile is similar to a simple shear flow: it satisfies the incompressibility condition, it does not produce any pressure gradient in the system, and the nonlinear term vanishes exactly for this profile. It is, therefore, an exact solution of the equations of motion (1) and (2), with its magnitude being set by the injection rate ε_W and the kinematic viscosity ν. In general, one can construct many exact solutions of the Navier-Stokes equations with $k = 1$, similar to the model profile discussed above, for which the nonlinear term vanishes. What is surprising, however, is that this self-organized large-scale state is dynamically connected to the isotropic turbulence at sufficiently low Reynolds numbers.

When the system selects this self-organized state, it stays there for as long as our simulations continue. Together with the fact that this state is dynamically selected by the system, it seems to imply that this state is linearly stable. In order to further probe this statement, we have performed exploratory simulations where we have perturbed the self-organized state with random perturbations and observed their evolution. For sufficiently small amplitude of the perturbations, simulations always returned to the self-organized state, while for larger perturbations the system became turbulent, as shown in Fig. 2 of the Supplemental Material [36]. Therefore, the simple state reported here has the same property as the laminar state in many wall-bounded parallel shear flows (cf. the Hagen-Poiseuille profile in pipe flow [37]): it is a linearly stable simple exact solution that can be destabilized by a finite-amplitude perturbation.

Next, we observe that at a fixed Reynolds number, the time of self-organization ($t/t_0 \approx 240$ in the example above) strongly depends on the initial conditions. We explore this variability systematically by starting 100 runs with different initial conditions for a fixed value of Re. In each simulation, we monitor the time evolution of the total energy $E(t)$ and the dissipation rate $\varepsilon(t) = 2\nu \int_{k_{\min}}^{k_{\max}} dk k^2 E(k,t)$. In order to identify the moment when the turbulent dynamics collapses onto the self-organized state, we employ a criterion that is based on the observation that since the kinetic energy in the self-organized state is confined to modes with $k = 1$, the asymptotic value E_∞ for all individual runs in a given ensemble (at a given Re) can be calculated from the energy input rate ε_W and ν. For statistically stationary flows the energy input rate ε_W must equal the dissipation rate ε, and we obtain for the total energy of the self-organized state

$$E_\infty = \frac{\varepsilon_W}{2\nu} = \text{const} \tag{5}$$

Our data confirm that in every simulation, the total energy eventually reaches the asymptotic value E_∞, and the self-organization time can be defined as the time when $E(t) = E_\infty$. We have checked that when we define the relaminarization moment as the time when the dissipation rate equals the input rate without any fluctuations, we obtain identical results.

We quantify the variability of the self-organization times by introducing a survival probability $P_{\mathrm{Re}}(t)$ that at a given Re gives the probability that the system is still turbulent at time t, having started in a turbulent state at time $t = 0$. For each t, we estimate this probability by dividing the number of runs that are still turbulent after time t by the total number of runs performed at this Reynolds number. The resulting survival probabilities are shown in Fig. 2 for a range of Re. We find that after some initial lag time during which the system has evolved from the initial condition into the turbulent state, the survival probability follows a simple exponential law

$$P_{\mathrm{Re}}(t) \sim \exp[-t/\tau(\mathrm{Re})], \tag{6}$$

where $\tau(\mathrm{Re})$ is the typical lifetime of turbulence that only depends on the Reynolds number. The exponential form of the survival probability suggests that the process is memoryless, i.e., at each time the rate of relaminarization is constant and does not depend on the previous dynamics of the system. This behavior is identical to what was observed in wall-bounded shear flows, such as pipe [9,10,13,17,38] or plane Couette flow [11,25,26]. There, it was attributed to the escape from a chaotic saddle associated with relaminarization of localized turbulence [17,18,38].

In order to verify that our results do not depend on the size of the simulation box, one ensemble of 100 runs was created using a larger simulation box with $L_{\mathrm{box}} = 4\pi$. The collapse of turbulence is also observed in these runs and leads to an exponential survival probability with the same characteristic lifetime as a reference data set at $L_{\mathrm{box}} = 2\pi$ [36].

The characteristic lifetime τ is obtained at each Reynolds number from fitting the survival probabilities to Eq. (6), see the solid lines in Fig. 2. We observe a steep increase in τ with increasing Reynolds number as shown in Fig. 3. To find the functional form $\tau = \tau(\mathrm{Re})$, we fit the observed lifetime to various model expressions. First, we consider a power law with an exponent $n < 0$ in the form $\tau \sim (\mathrm{Re}_c - \mathrm{Re})^n$ that would suggest a divergence of the lifetime at some critical Reynolds number Re_c. We find that it is not compatible with the data for any value of n; Fig. 3 shows an example with $n = -1$. The same applies to an exponential increase of τ with Re. However, we find that a superexponential scaling in the form

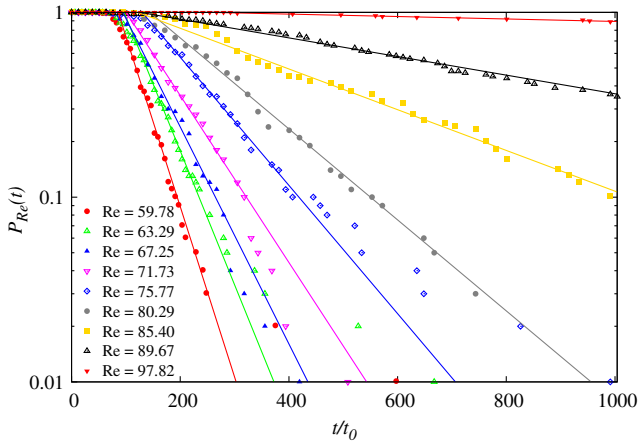

FIG. 2 (color online). Survival probability as a function of the dimensionless time t/t_0 from the beginning of a simulation.

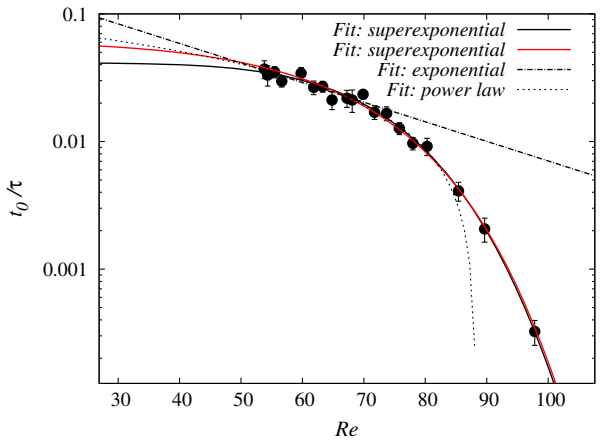

FIG. 3 (color online). Reynolds number dependence of the escape rate t_0/τ. The red (gray) line is a two-parameter fit of the expression $t_0/\tau(\mathrm{Re}) = 0.064 \exp[-\exp(a + b\mathrm{Re})]$, the black line is a two-parameter fit of the expression $t_0/\tau(\mathrm{Re}) = \exp[a' - (b'\mathrm{Re})^{5.6}]$), the dash-dotted line is a fit of an exponential, and the faint dotted line is a fit of a linear dependence of t_0/τ on Reynolds number.

$$\frac{\tau(\mathrm{Re})}{t_0} = c \exp\left[\exp(a + b\mathrm{Re})\right] \tag{7}$$

is compatible with our data for a fixed amplitude $c = 15.63$ and $a = -3.48 \pm 0.51$, $b = 0.052 \pm 0.005$, see Fig. 3. Once again, this conclusion parallels the superexponential scaling of the lifetimes in wall-bounded shear flows [9,18,38]. Further support for this scaling is provided in the Supplemental Material [36].

We note that the superexponential law (7) is not the only possible form that produces an acceptable fit to the data. Another superexponential dependence, $\tau(\mathrm{Re})/t_0 = \exp[-a' + (b'\mathrm{Re})^{5.6}]$ with $a' = -3.18 \pm 0.14$ and $b' = 0.0136 \pm 0.0003$ also gives a good agreement with the data set, as can be seen in Fig. 3.

The results presented in this Letter show that there is a surprising analogy between the behavior of the isotropic turbulence forced at a large scale and wall-bounded shear flows at low Reynolds numbers. We observe that there is a spontaneous transition from turbulence to a spatially simple state, which we have identified here, and this "laminar" state is linearly stable but can be destabilized by a finite-amplitude perturbation. The turbulent-laminar transition is abrupt and memoryless, and the associated survival probability is exponential in time, cf. Refs. [9,10,13,16,17,38]. The turbulent lifetimes do not diverge with an increase in Re, but instead grow superexponentially, cf. Refs. [38,39]. This analogy implies that the phenomena of the transition to turbulence in wall-bounded shear flows and forced isotropic turbulence, typically thought of as a high-Re phenomenon away from boundaries, are dynamically similar and can be understood within the same theoretical framework. As recent research suggests, the transition to turbulence in shear flows belongs to the directed percolation universality class [26,40–42], and we argue that the same might be valid for forced isotropic turbulence.

The phase space of turbulent wall-bounded shear flows is organized by exact solutions and periodic orbits of the Navier-Stokes equations [43,44] and the relaminarization events are associated with a sudden escape from this part of the phase space [16]. Since we observe the same phenomenology, we speculate that the phase space of the forced isotropic turbulence should also be organized by coherent structures (exact solutions and periodic orbits). In Fig. 4 we plot the energy content in the $k = 2$ mode versus the energy in the $k = 1$ mode for a run at $\mathrm{Re} = 76.86$. Each point there corresponds to a particular moment in time and the dynamics proceeds from left to right, until the system relaminarizes (i.e., $E_1 = E_\infty$ and $E_2 = 0$). We observe that the dynamics revolves around several points in phase space that are very suggestive of exact unstable solutions [44]. Identification of these coherent states will be the subject of future work.

This work also suggests that the type of forcing employed here is well suited for DNS of isotropic turbulence with a view of creating an artificial, simpler system whose dynamics still resemble more complicated real physical systems, such as shear flows. Other types of forcing, notably various forms of stochastic forcing, are routinely used but might not have the phenomenological similarities with the transition to turbulence in wall-bounded shear flows. Recent results on self-organization in magnetohydrodynamic flows, for example, demonstrate that introducing random phases in the forcing term precludes the formation of a large-scale flow [24]. We argue that Eq. (3) gives in fact a better approximation to naturally occurring turbulence than an explicitly stochastic (and thus more costly) forcing.

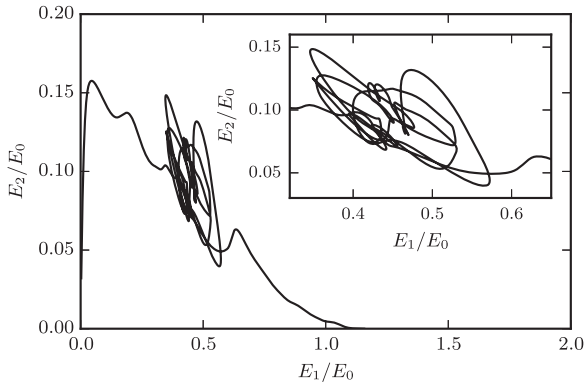

FIG. 4. Phase portrait E_2 vs E_1 for $\mathrm{Re} = 76.86$. Each point corresponds to a particular moment in time. All energies are scaled with the initial total kinetic energy E_0. Inset: enlargement of the turbulent region of the main graph showing that the dynamics is organized by several points in phase space suggestive of unstable exact solutions.

Our results provide new potential targets for turbulence control, since we have shown that there is a stable large-scale state hidden in what appears to be isotropic turbulence. A particular choice of an additional external force may be sufficient to push the system into the basin of attraction of this stable state.

We would like to thank Bruno Eckhardt, W. David McComb, Arjun Berera, and Samuel Yoffe for helpful discussions, and Bernardas Jankauskas and Richard Ho for initial help with simulations. This work has made use of the resources provided by the Edinburgh Compute and Data Facility. M. F. L. and A. M. acknowledge support from the U.K. Engineering and Physical Sciences Research Council (EP/K503034/1 and EP/I004262/1).

*m.linkmann@ed.ac.uk

[1] A. G. Darbyshire and T. Mullin, J. Fluid Mech. **289**, 83 (1995).

[2] B. Hof, C. W. H. van Doorne, J. Westerweel, F. T. M. Nieuwstadt, H. Faisst, B. Eckhardt, H. Wedin, R. R. Kerswell, and F. Waleffe, Science **305**, 1594 (2004).

[3] M. Nishi, B. Ünsal, F. Durst, and G. Biswas, J. Fluid Mech. **614**, 425 (2008).
[4] Y. Duguet, P. Schlatter, and D. S. Henningson, Phys. Fluids **21**, 111701 (2009).
[5] F. Mellibovsky, A. Meseguer, T. M. Schneider, and B. Eckhardt, Phys. Rev. Lett. **103**, 054502 (2009).
[6] T. M. Schneider, D. Marinc, and B. Eckhardt, J. Fluid Mech. **646**, 441 (2010).
[7] Y. Duguet, P. Schlatter, D. S. Henningson, and B. Eckhardt, Phys. Rev. Lett. **108**, 044501 (2012).
[8] M. Avila, F. Mellibovsky, N. Roland, and B. Hof, Phys. Rev. Lett. **110**, 224502 (2013).
[9] B. Hof, J. Westerweel, T. M. Schneider, and B. Eckhardt, Nature (London) **443**, 59 (2006).
[10] K. Avila, D. Moxey, A. de Lozar, M. Avila, D. Barkley, and B. Hof, Science **333**, 192 (2011).
[11] A. Schmiegel and B. Eckhardt, Phys. Rev. Lett. **79**, 5250 (1997).
[12] H. Faisst and B. Eckhardt, J. Fluid Mech. **504**, 343 (2004).
[13] M. Avila, A. P. Willis, and B. Hof, J. Fluid Mech. **646**, 127 (2010).
[14] J. P. Crutchfield and K. Kaneko, Phys. Rev. Lett. **60**, 2715 (1988).
[15] U. Brosa, J. Stat. Phys. **55**, 1303 (1989).
[16] E. Ott, *Chaos in Dynamical Systems*, 2nd ed. (Cambridge University Press, Cambridge, England, 2002).
[17] B. Eckhardt, T. M. Schneider, B. Hof, and J. Westerweel, Annu. Rev. Fluid Mech. **39**, 447 (2007).
[18] B. Eckhardt, H. Faisst, A. Schmiegel, and T. M. Schneider, Phil. Trans. R. Soc. A **366**, 1297 (2008).
[19] B. Eckhardt and T. M. Schneider, Eur. Phys. J. B **64**, 457 (2008).
[20] L. Xi and M. D. Graham, Phys. Rev. Lett. **104**, 218301 (2010).
[21] L. Xi and M. D. Graham, J. Fluid Mech. **693**, 433 (2012).
[22] A. S. Monin and A. M. Yaglom, *Statistical Fluid Mechanics*, 2nd ed. (MIT Press, Cambridge, MA, 1975).
[23] W. D. McComb, M. F. Linkmann, A. Berera, S. R. Yoffe, and B. Jankauskas, J. Phys. A **48**, 25FT01 (2015).
[24] V. Dallas and A. Alexakis, Phys. Fluids **27**, 045105 (2015).
[25] S. Bottin and H. Chaté, Eur. Phys. J. B **6**, 143 (1998).
[26] L. Shi, M. Avila, and B. Hof, Phys. Rev. Lett. **110**, 204502 (2013).
[27] S. R. Yoffe, Ph.D. thesis, University of Edinburgh, 2012, arXiv:1306.3408.
[28] J. Jiménez, A. A. Wray, P. G. Saffman, and R. S. Rogallo, J. Fluid Mech. **255**, 65 (1993).
[29] W. D. McComb, A. Hunter, and C. Johnston, Phys. Fluids **13**, 2030 (2001).
[30] Y. Yamazaki, T. Ishihara, and Y. Kaneda, J. Phys. Soc. Jpn. **71**, 777 (2002).
[31] Y. Kaneda, T. Ishihara, M. Yokokawa, K. Itakura, and A. Uno, Phys. Fluids **15**, L21 (2003).
[32] W. D. McComb and A. P. Quinn, Physica (Amsterdam) **317A**, 487 (2003).
[33] W. D. McComb, S. R. Yoffe, M. F. Linkmann, and A. Berera, Phys. Rev. E **90**, 053010 (2014).
[34] W. D. McComb, A. Berera, S. R. Yoffe, and M. F. Linkmann, Phys. Rev. E **91**, 043013 (2015).
[35] Y. Kaneda and T. Ishihara, J. Turbul., **7**, N20 (2006).
[36] See Supplemental Material at http://link.aps.org/supplemental/10.1103/PhysRevLett.115.134502 for simulation details and further analyses discussed in the text.
[37] P. Drazin and W. Reid, *Hydrodynamic Stability* (Cambridge University Press, Cambridge, England, 2004).
[38] B. Hof, A. de Lozar, D. J. Kuik, and J. Westerweel, Phys. Rev. Lett. **101**, 214501 (2008).
[39] N. Goldenfeld, N. Guttenberg, and G. Gioia, Phys. Rev. E **81**, 035304 (2010).
[40] M. Sipos and N. Goldenfeld, Phys. Rev. E **84**, 035304 (2011).
[41] L. Shi, M. Avila, and B. Hof, arXiv:1504.03304.
[42] H.-Y. Shih, T.-L. Hsieh, and N. Goldenfeld, arXiv:1505.02807.
[43] H. Faisst and B. Eckhardt, Phys. Rev. Lett. **91**, 224502 (2003).
[44] P. Cvitanović and J. F. Gibbon, Phys. Scr. **T142**, 014007 (2010).